THE UNIVERSITY of EDINBURGH

Edinburgh Research Explorer

Tunable Graphene-Polymer Resonators for Audio Frequency Sensing Applications

Citation for published version:
Al-masha'al, AKE, Wood, G, Torin, A, Mastropaolo, E, Newton, MJ & Cheung, R 2019, 'Tunable Graphene-Polymer Resonators for Audio Frequency Sensing Applications', *IEEE Sensors Journal*, vol. 19, no. 2, pp. 465-473. https://doi.org/10.1109/JSEN.2018.2877463

Digital Object Identifier (DOI):
10.1109/JSEN.2018.2877463

Link:
Link to publication record in Edinburgh Research Explorer

Document Version:
Peer reviewed version

Published In:
IEEE Sensors Journal

General rights
Copyright for the publications made accessible via the Edinburgh Research Explorer is retained by the author(s) and / or other copyright owners and it is a condition of accessing these publications that users recognise and abide by the legal requirements associated with these rights.

Take down policy
The University of Edinburgh has made every reasonable effort to ensure that Edinburgh Research Explorer content complies with UK legislation. If you believe that the public display of this file breaches copyright please contact openaccess@ed.ac.uk providing details, and we will remove access to the work immediately and investigate your claim.

Download date: 07. May. 2023

Tunable Graphene-Polymer Resonators for Audio Frequency Sensing Applications

Asaad K. Al-mashaal, Graham S. Wood, *Member, IEEE,* Alberto Torin, Enrico Mastropaolo, Michael J. Newton, and Rebecca Cheung, *Senior Member, IEEE*

***Abstract*— Suspended vibrating membranes play a vital role as structural elements in electromechanical resonators and form the foundation of modern acoustic transducers. The realization of large scale mechanical resonators based on large and thin membranes, however, still faces several challenges. In this work, a simple and reproducible process has been developed to transfer millimeter-scale circular and square membranes composed of ~2.5 nm of graphene and a thin film of ~ 370 nm of poly(methyl methacrylate) (PMMA). The uniqueness of the demonstrated fabrication technique is the ability to produce high yield and non-ruptured suspended membranes with exceptional diameter (side length) to thickness aspect ratios of ~ 10,000. One of the perceived advantages of building a mechanical resonator from a bilayer structure, in which materials have different mechanical and thermal properties, is that such a structure can enable the use of electrothermal transduction to drive the resonator into resonance and tune its resonant frequencies. Due to the large area of the fabricated membranes, resonant frequencies within the audio range have been obtained. The frequency tuning response of circular and square membranes has been found to be influenced significantly by the magnitude of the applied voltage. A downward shift of the resonant frequency and an increase of the amplitude of vibration have been observed in response to the increase of the applied DC and AC voltages. The demonstrated fabrication technique and tuning mechanism could be employed as a platform for potential acoustic and audio applications.**

***Index Terms*—Audio resonator, bilayer membrane, electro-thermal tuning, graphene, PMMA.**

I. Introduction

THE practical use of acoustic devices has been expanded to cover a wide range of applications including, but not limited to, microphones, earphones, loudspeakers, and hearing aids. Most modern acoustic transducers use membrane-like structures (i.e. a diaphragm) as vibrating elements to convert one form of energy into another. The overall performance of a vibrating membrane is determined by its design, material's properties and driving/actuation mechanism. For audio sensing applications, the membrane should be designed in such a way that the audible frequency range (20 Hz – 20 kHz) is covered. Various shapes of vibrating membranes have been created including rectangular, square and perforated designs. However, the circular shape is the most popular design for the membrane of modern microphones [1]. From a materials standpoint, different types of materials have been used as structural membranes for audio transducers. For instance, most existing microphones use membranes made from silicon, silicon nitride, and polysilicon [2]. In addition to the use of silicon-based materials, cochlear implant devices utilize membranes made of piezoelectric materials such as lead zirconate titanate (PZT), aluminum nitride (AlN), polyvinylidene fluoride (PVDF), and fluoride trifluoroethylene (P(VDF-TrFE)) [3]. However, the traditional materials used in the commercial audio transducers have some drawbacks related to the material properties such as flexibility, strength, stress, and compatibility. An alternative material that has attracted great attention in both academia and industry is the carbon-based material of graphene. Graphene is an extraordinary two-dimensional (2D) material that has shown superiority over other known materials in the field of micro- and nanoelectromechanical systems (MEMS/NEMS) due to its exceptional properties. For example, a few studies have been reported recently using graphene-based membranes to realize audio transducers including a loudspeaker [4], microphones [5]–[7], and earphones [8], [9]. However, the membrane used in these studies is either relatively thick (more than 60 layers), which might possibly inherit the properties of graphite instead of graphene, or it is transferred and attached to a thick supported substrate.

To exploit the outstanding properties of graphene thin-films in resonators-based devices, a thin-film of graphene sheet is required to be isolated from its growth substrate and suspended freely. From the fabrication point of view, however, making defects-free and large-area suspended membranes of graphene is extremely challenging. Mechanically, a thin-film of mono or multilayer graphene is sufficiently fragile that it can be wrinkled or ruptured easily during the fabrication process. The challenge becomes even greater with the increase of graphene sheet area. The most critical step in the fabrication process is to transfer graphene from its growth substrate to the substrate of

Manuscript received July 05, 2018. This work was supported in part by Engineering and Physical Sciences Research Council (EPSRC). The Ministry of Higher Education and Scientific Research (MOHESR) of Iraq is acknowledged for the financial support through the PhD scholarship program.

A. Al-mashaal, G. S. Wood, E. Mastropaolo and R. Cheung are with the School of Engineering, Institute for Integrated Micro and Nano Systems, The University of Edinburgh, Edinburgh, UK. (e-mail: asaad.al@ed.ac.uk; asaad.edaan@uobasrah.edu.iq; g.s.wood@ed.ac.uk; e.mastropaolo@ed.ac.uk; r.cheung@ed.ac.uk).

A. Torin and M. J. Newton are with the Edinburgh College of Art, Reid School of Music, Acoustics and Audio Group, The University of Edinburgh. (e-mail: A.Torin@ed.ac.uk; Michael.Newton@ed.ac.uk).

interest without damaging the graphene membrane or the surface of the target substrate. Despite all the enormous efforts that have been made on the developments of graphene synthesis and transfer methods, there are still undoubtedly a number of challenges facing the production of high-quality graphene films on a large scale. The difficulties appear when processes such as solvent rinsing or dry annealing are involved in the fabrication. The graphene films prepared by currently available approaches [10]–[13] suffer from many problems, most of which are: small size, low yield, residue defects, sagging, buckling, folding, and rupturing. Therefore, the possible solutions to overcome these issues are either increasing the thickness of the membrane or reducing its size (area). However, increasing the membrane's thickness might have an influence on the output performance of the device in such a way that leads to a decrease in the vibration displacement and sensitivity [5]. In addition, one of the main limitations of reducing the vibrating structures dimensions to the nano- and micro-scale is that these micro and nanodevices can operate at high-frequency dynamic range (*i.e.* MHz - GHz) only [14]–[16]. Such devices will not be suitable for audio frequency applications. Another outstanding challenge in graphene-based devices is driving them into resonance and tuning their frequencies over a desired range. Although electrostatic actuation is the most widely used method of driving in the vast majority of existing graphene-based resonators [17], [18], issues such as design complexity, large driving voltage, nonlinearity, short circuiting, and pull-in instability are the main drawbacks associated with this actuation approach.

In this study, we aim to address the following issues: the ability to fabricate/transfer successfully an ultra-large and thin film of graphene using a damage-free transfer technique, to achieve an operating frequency within the audio range using electrothermal transduction mechanism, and to make graphene-based membranes tunable over a desired range of frequencies with a relatively small tuning voltage. Therefore, a simply designed resonator made from ultra-large graphene-polymer membranes has been demonstrated in this study. First, to enable the graphene-based resonator to be operated at low frequency regime (*e.g.* 20 Hz – 20 kHz), large membranes on macro-scale size with large aspect ratio of area to thickness have to be suspended over a cavity. We have demonstrated a simple and reproducible fabrication technique to transfer large graphene-based circular membranes with a diameter of 3.5 mm and square membranes with a side length of 3 mm on top of a cavity. In this technique, a thin film of poly(methyl methacrylate) (PMMA) has been attached to the graphene sheet to act as a mechanical supporting layer during and after the transfer process. The PMMA thin film will not be removed after the transfer, thus the final structure of the resonator will be in the form of a bilayer membrane.

In addition, to overcome the limitations associated with the existing electrostatic and other actuation/tuning approaches, electrothermal transduction has been employed as an alternative option. In particular, graphene possesses superior thermal conductivity ($\sim 2000 - 5300$ W/mK) [19], [20] and negative coefficient of thermal expansion ($\sim -7 \times 10^{-6}$ K^{-1}) [19], which allow graphene-based mechanical resonators to be actuated and tuned electrothermally. Electrothermal actuation of a bilayer system relies on the difference in the coefficient of thermal expansion for different materials.

In general, the main advantage of using bilayer membranes, which are made from an ultra-thin sheet of graphene with high strength and durability and a thin layer of PMMA that has lower density and elasticity than graphene, is to enhance the durability of the bilayer structure, and lower the frequency of operation. Also, unlike conventional materials in audio sensing, graphene is known for its low heat capacity per unit area and high thermal conductivity, which can induce joule heating more effectively. In such a case, better performance with sufficient sensitivity is expected for graphene-based resonators. Moreover, frequency tuning and tuning sensitivity of graphene-polymer membranes have not been investigated comprehensively in the literature. Frequency tuning is of great value to audio transducers, especially for hearing aids as well as for other sensing applications such as terahertz modulators [21], self-sustained oscillators [17], plasmonic filters [22], and frequency mixers [23]. Importantly, we show in this work that the electrothermal transduction can be used to tune the resonant frequency of the bilayer membranes and increase their vibration amplitude with relatively small tuning voltages. Compared to other audio transducers that require high voltage (*e.g.* 100 V [4], 200 V [7]) for operation, the tuning voltage range used in this work is significantly smaller (i.e. 1 – 9 V).

II. Experimental Section

A. Preparation of desired substrate

Fig. 1 shows a schematic diagram of the process flow for the fabrication of the target substrate. First, a dielectric layer of 250 nm of silicon dioxide (SiO_2) has been deposited on a p-type silicon substrate by chemical vapor deposition (fig. 1a). To create electrode pads for electrothermal actuation/tuning, a layer of 500 nm of aluminum metal has been deposited on top using a DC sputtering system and patterned by a lift-off process

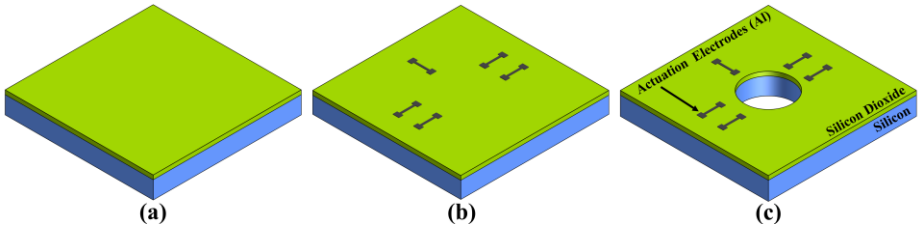

Fig. 1. Schematic diagram of the fabrication process for the desired substrate of graphene-PMMA resonator: (a) SiO_2 deposited, (b) Al sputtered and patterned, (c) SiO_2/Si etched and cavities created.

(fig. 1b). After spin coating and patterning of photoresist, circular cavities with a diameter of 3.5 mm and depth of 380 µm have been created via deep reactive ion etching (DRIE) by etching the oxide layer and through the whole depth of the silicon substrate (fig. 1c). The same procedure described above has been applied to create square cavities with a side length of 3 mm.

B. *Transfer of graphene-PMMA membrane*

Fig. 2 shows a schematic illustration of the transfer process of graphene-PMMA membrane to the target substrate. In this work, a multilayer (~ 2.5 nm) graphene film synthesized on copper foil by chemical vapor deposition (CVD) has been used. To support the graphene sheet during and after the transfer, a thin layer of ~ 375 nm of PMMA (molecular weight ~996000 with a concentration of 4% in chlorobenzene) has been spin coated and annealed at 80 °C for 5 minutes (fig. 2a). The sample has been left for 24 hours to dry fully in a cleanroom environment. Next, copper etchant solution of ferric chloride ($FeCl_3$) has been used to etch the copper foil (fig. 2b). After being cleaned by rinsing in deionized water (DIW) many times, the floating graphene-PMMA membrane has been scooped out and transferred to the target substrate. Since the transferred membrane is suspended over an open cavity, a water droplet will be trapped into the cavity, and due to capillary effects, this may cause a rupture of the transferred membrane. Here, we have used a simple and effective technique that can tackle such stiction-related failures. For this step, two metal bars with an appropriate height (e.g. 30 mm) are placed securely on a hotplate at 80 °C. Then, the entire stack of graphene-PMMA-substrate was placed on the metal bars creating a bridge-like structure (fig. 2c). In this case, the stack will not be in direct contact with the hotplate, and instead the heating that comes from the hotplate will dry the sample slowly until the water liquid is evaporated completely. After this step, the membrane-bearing substrates samples have been transferred to another hotplate and annealed at 140 °C for 10 – 20 seconds to stretch the suspended membrane over the cavity (fig. 2d). As shown in figure 3, this technique leads to a feasible production of ultra-large bilayer membranes without causing a rupture of the entire membrane or burning the PMMA supporting layer.

III. Results and Discussion

A. *Characterization and testing setup*

Fig. 3a shows an optical image of the transferred graphene-PMMA membrane suspended over a square cavity with a side length of 3 mm. A scanning electron microscope (SEM) image of the square membrane in contact with the actuation electrode is shown in fig. 3b. The membranes have been driven into resonance by applying an input AC voltage superimposed on a DC bias voltage to the actuation electrodes. Under atmospheric pressure and room temperature conditions, the dynamic vibration of both circular and square membranes have been detected optically using a laser Doppler vibrometer (LDV). Since the most sensitive audio frequencies of the audible region are located within the range of 10 Hz – 8 kHz, the LDV results reported in this work are limited to the fundamental frequency within that range only. Therefore, an excitation signal has been swept through the frequency range of interest (10 Hz–8 kHz) while applying a discrete Fourier transform (FFT) to the excitation signal. Moreover, the amplitude of vibration has been measured experimentally by applying a sinusoidal excitation signal at the resonant frequency. To investigate the dynamic tuning of the membranes using electrothermal transduction, the resonant frequencies and amplitude of vibration have been monitored while changing the applied input voltage. For all measurements, the input voltages have been applied between the tuning electrodes labelled 2 and 5 in fig. 2d. It is expected in a such scenario that the electrical current will flow through the center area of the suspended membrane, targeting the anti-nodal points of the fundamental resonant mode and consequently maximizing the vibration amplitude [24].

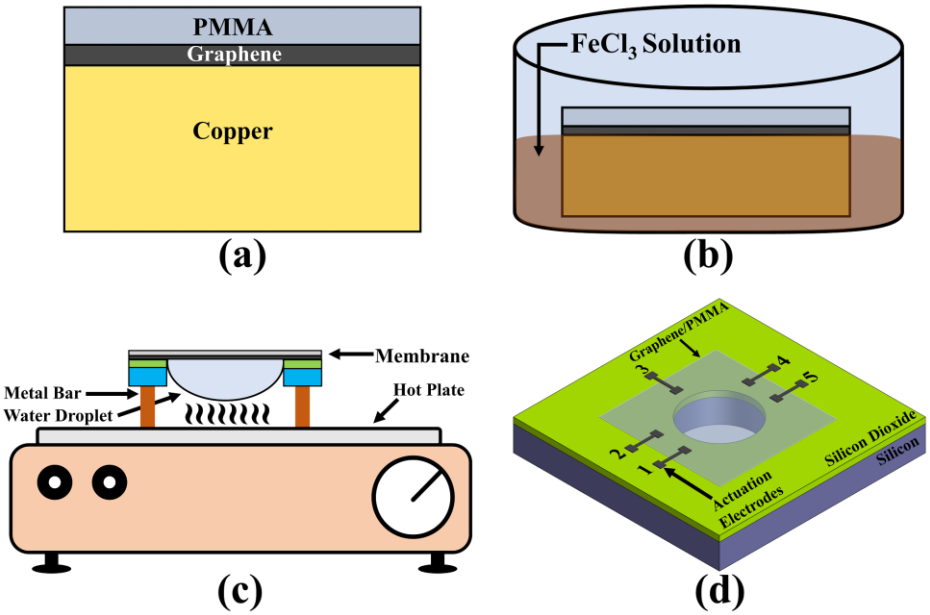

Fig. 2. Schematic illustration of the transfer process of graphene-PMMA on a substrate with 3.5 mm-diameter circular cavities. (a) PMMA spin coated on graphene/copper. (b) Copper foil etched in $FeCl_3$. (c) Water evaporated from transferred membrane. (d) Final structure of graphene-PMMA resonator.

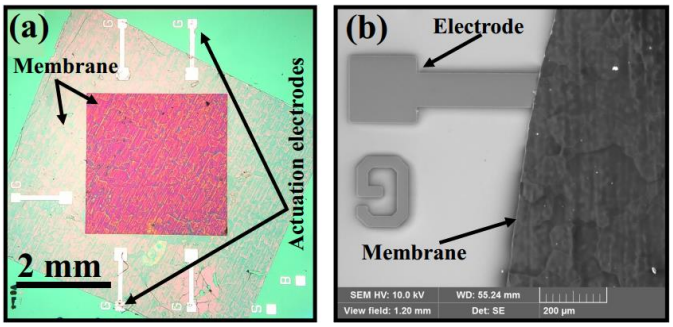

Fig. 3. (a) Optical micrograph of the suspended membrane over a square cavity, and (b) SEM image of the membrane in contact with the actuation/tuning electrode.

B. *Dynamic tuning: frequency spectra*

To investigate the dynamic tuning of graphene-PMMA membranes using electrothermal transduction, a combination of different AC and DC voltages have been applied to the actuation/tuning electrodes. The electrothermal tuning has been performed for both circular and square resonators. First, the AC voltage has been kept constant at an amplitude of 1 V while sweeping the DC tuning voltage from 1 to 9 V. Second, the DC voltage has been held at 1 V while varying the applied AC voltage from 1 to 9 V. The frequency response of the membranes to the applied voltages is shown in fig. 4.

In general, with the application of electrothermal tuning voltages of 1 – 9 V, the frequency response of both circular and square membranes has been found to be linear, which can be seen from the symmetric curves of resonance shown in fig.4. Such good linearity is likely to be related to the relatively small tuning voltages used in our resonator devices. The possibility for graphene-PMMA membranes to exhibit nonlinear effects when applying tuning voltages higher than 10 V is not covered in this work. From the entire frequency spectra measurements shown in fig. 4, it can be observed clearly that the increase of the applied voltage (DC or AC) leads to a downward shift of the fundamental resonant frequency accompanied by an increase of the amplitude of vibration. For example, the resonant frequency of circular and square membranes has been found to shift downward maximally by ~ 9 % and ~ 5 % respectively in response to a DC tuning voltage of 9 V. The measurements of the vibration amplitude of circular and square membranes as a function of the applied voltage is shown in fig. 5.

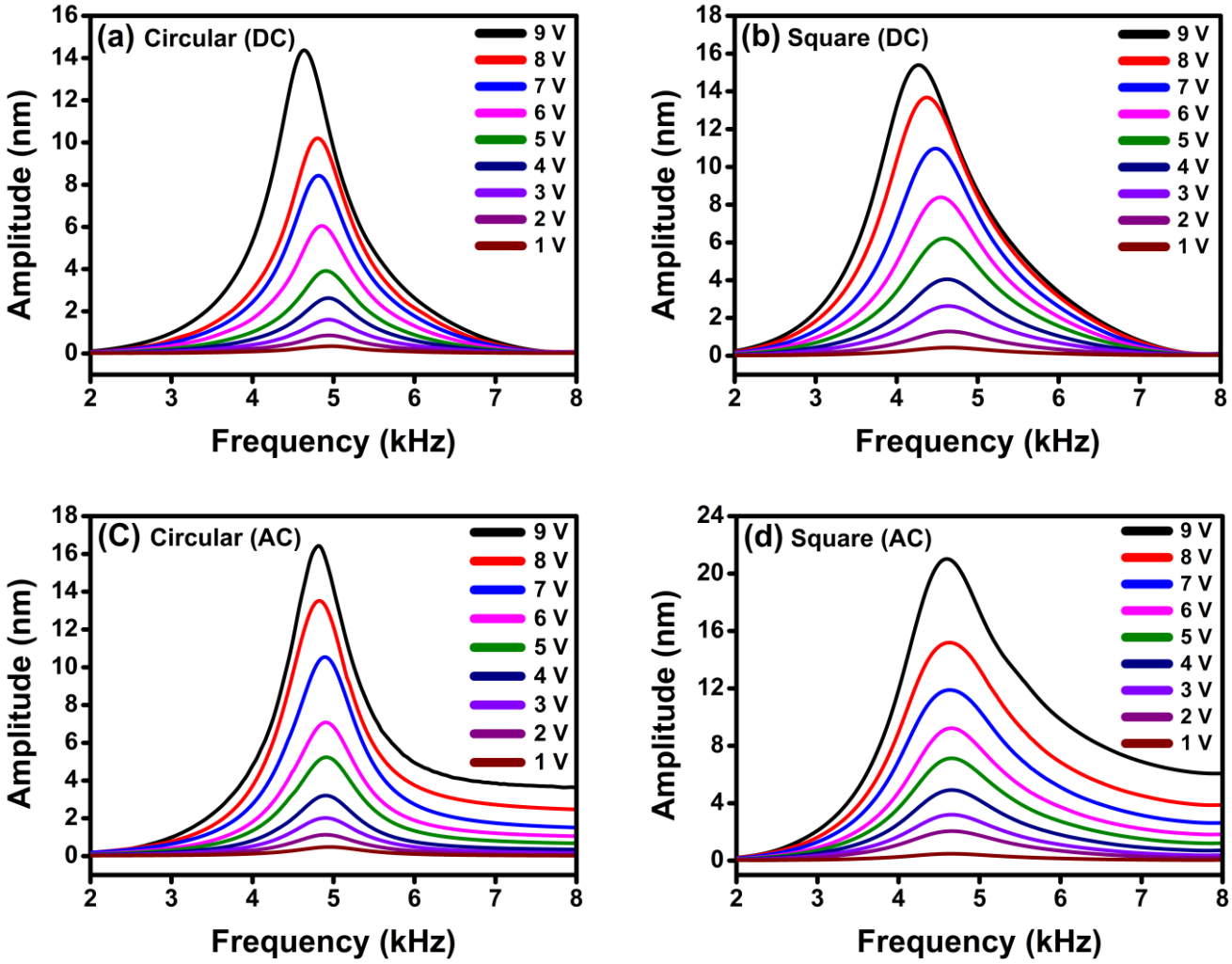

Fig. 4. Measured amplitude of vibration versus resonant frequency shift for circular and square membranes with respect to the applied voltage. (a, b) Frequency response measured at a constant AC voltage of 1 V and a DC tuning voltage ranging from 1 to 9 V. (c, d) Frequency response measured at a DC voltage fixed at 1 V and an AC tuning voltage varying from 1 to 9 V.

C. Tuning sensitivity

To evaluate the efficiency of the electrothermal tuning used in this work, the tuning sensitivity of our bilayer membranes has been estimated based on the experimental data obtained from frequency response measurements. The insets in fig. 5 depict the tuned resonant frequency (f) measured at different amplitudes (1 – 9 V) of the applied AC and DC voltages. The fitted linear curves in the insets represent the estimated tuning sensitivity ($\Delta f / \Delta V$) of the measured devices.

Overall, a significant influence of the applied voltage amplitude on the frequency tuning response has been observed for both circular and square membranes. This effect can be seen clearly in two ranges of the applied voltage: the first range is from 1 to 5 V and the second range is from 5 to 9 V. In general, the amplitude of vibration and tuning sensitivity have been observed to be higher in the second range compared to the first range.

In case of the circular membranes, it has been found that increasing the DC tuning voltage in the first range of 1 – 5 V leads to a vibration amplitude of ~ 8 nm/V accompanied by a tuning sensitivity of 18 Hz/V, see fig. 5a. In the second range of 5 – 9 V, however, the amplitude of vibration and tuning sensitivity have been found to be about three times and two times greater, respectively, than in the first range. For frequency tuning under different AC voltages, similar behavior to the DC case has been observed (fig. 5c). Both the amplitude of vibration and tuning sensitivity are observed to be greater by three times in the second range of the applied AC voltage than that in the first range. Therefore, it is deduced that the circular membranes exhibit higher vibration amplitude and better tuning sensitivity in the second range of 5 – 9 V of the applied voltage. In addition, by considering the overall trend of the observed response from the first to the second range, the applied AC voltage seems to be more influential in this regard.

In case of the square membranes, an amplitude of vibration of ~ 1.28 nm/V and a tuning sensitivity of 23 Hz/V have been achieved in the first range of the DC tuning voltage (fig. 5b). Comparatively, the implementation of the DC tuning in the second range would make the square membranes exhibit a vibration amplitude of 2.4 nm/V and tuning sensitivity more than three times larger. When different AC voltages are applied (fig. 5d), the observed behavior is almost similar to the DC tuning case, as the second range of the applied AC voltage results in an increase of the vibration amplitude of 3.4 nm/V compared to ~ 1.3 nm/V in the first range. The tuning sensitivity in the second range has been found to be more than three times greater than that in the first range. It is concluded therefore that the performance of the electrothermal tuning of the square membranes shows relatively larger vibration amplitude and

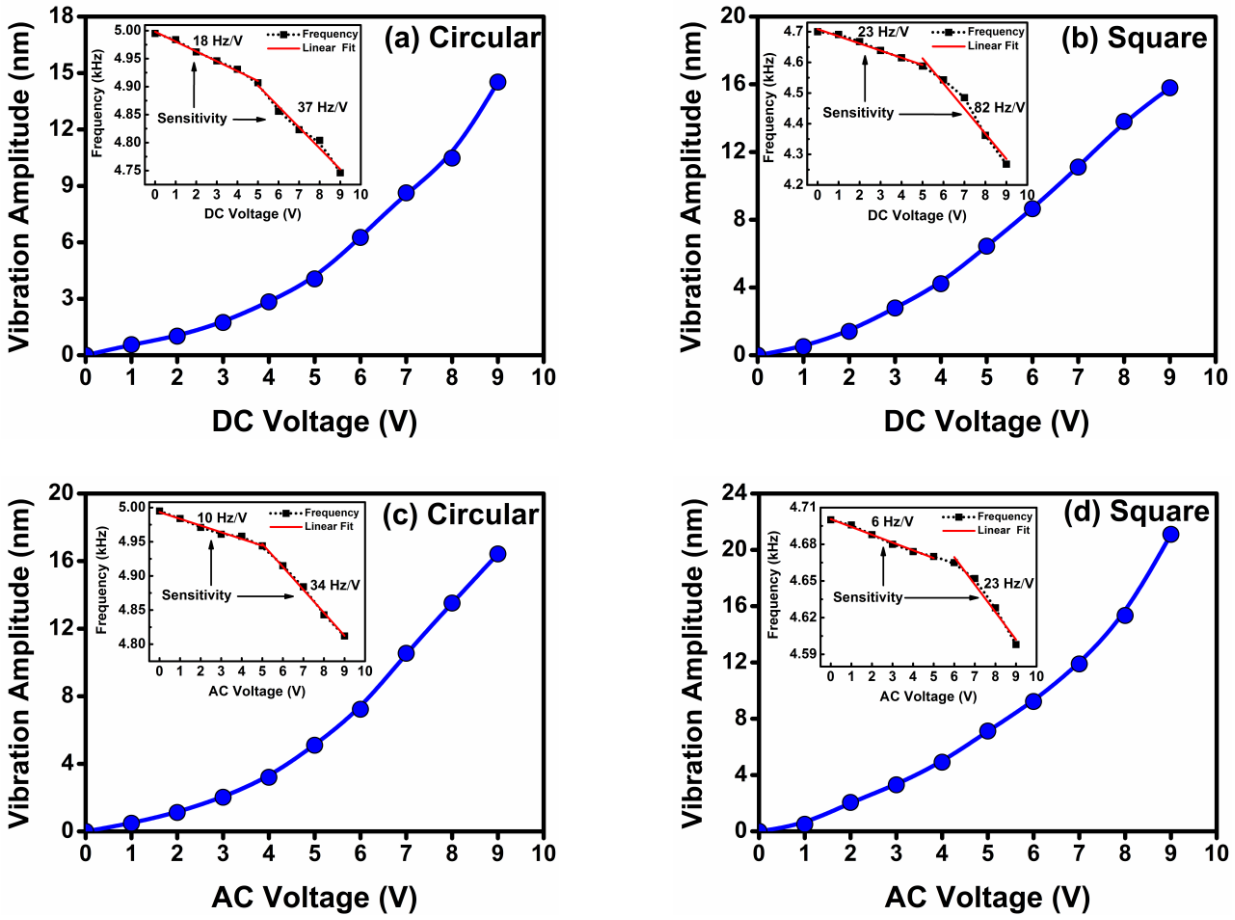

Fig. 5. Vibration amplitude of circular and square membranes as a function of the applied voltage (a, b) DC and (c, d) AC. Insets are the tuning sensitivity of the membranes estimated from frequency shift with respect to the applied voltage.

better tuning sensitivity in the second range for both DC and AC applied voltages.

In general, the highest tuning sensitivity of 82 Hz/V has been induced in the square membrane in the second range of the DC tuning voltage, while the largest amplitude of vibration of ~ 22 nm has been achieved for the square membrane at an AC voltage of 9 V. From the electrothermal tuning observations accomplished in this work, it can be concluded that it is more effective to perform the frequency tuning of the graphene-PMMA bilayer membranes under a DC bias voltage rather than an AC voltage. These results are consistent with other studies reported for electrothermally actuated silicon carbide MEMS resonators [25]. From the device design point of view, the square membranes have shown better tuning sensitivity than the circular ones when different DC bias voltages are applied. On the other hand, both the circular and square membranes show almost similar behavior under the application of an AC voltage.

It is worth pointing out that the measured quality (Q) factor of our bilayer resonators is relatively small (i.e. ~ 8 for circular membranes and ~ 5 for square membranes). It is believed that the small Q observed here is due to several sources of energy dissipation such as air damping, thermoelastic damping, anchor and surface losses, membrane size, and possibly modal frequency [26], [27].

D. Effect of tension

In the electrothermal tuning of the graphene-PMMA bilayer structures, a downward shift of the resonant frequencies and an increase of the amplitude of vibration for circular and square membranes have been observed. This dynamic tuning behavior is likely to be related to the membrane tension. In general, the in-plane pre-tension is dominant in the membrane structure while its out-of-plane bending rigidity can be negligible. However, in addition to the pre-tension (N_i) that can be considered as a built-in tension at room temperature, a thermal tension (N_t) can be induced in the membrane from the Joule heating during electrothermal actuation/tuning. Therefore, by taking into account the built-in tension as well as the thermally induced tension, the resonant frequencies of the circular and square membranes can be expressed as follows:

$$f_{mn}\,(circular) = \frac{\alpha_{mn}}{2\pi R}\sqrt{\frac{N_i + N_t}{\rho_{eff}\ t_{eff}}} \tag{1}$$

$$f_{mn}(square) = \frac{\beta_{mn}}{2\pi a}\sqrt{\frac{N_i + N_t}{\rho_{eff}\ t_{eff}}} \tag{2}$$

where R and a are respectively the radius and side length of the membrane, t_{eff} and ρ_{eff} are respectively the effective thickness and density of the bilayer membrane materials [24], and α_{mn} and β_{mn} are the dimensionless coefficients of the resonant mode (m and n are the number of nodal lines). From these equations, it can be seen that any variation in the membrane tension results in a shift of the resonant frequency. In order to estimate the magnitude of tension induced in the membranes, different values of resonant frequencies obtained from measurements have been applied in equations 1 and 2. Hence, the tension of circular and square membranes have been calculated and plotted in fig. 6a. The analytical calculations are based on the following parameters of circular (α_{01}= 2.405, R = 3.5 mm, ρ_{eff} = 1.05 × 10^3 Kg/m^3, t_{eff} = 373 nm) and square (β_{01}= 4.443, a = 3 mm, ρ_{eff} = 1.05 × 10^3 Kg/m^3, t_{eff} = 373 nm) membranes.

Fig. 6a shows a clear decrease in the membranes tension with the increase of the tuning voltage. The tension of circular membrane has been found to decrease from ~ 1.9 N/m at 1 V to ~ 1.7 N/m at DC tuning voltage of 9 V. The tension reduction of the square membrane, on the other hand, has been found to be relatively larger. For example, the square membrane shows tension reduction of ~ 0.4 N/m as the DC tuning voltage increases from 1 to 9 V. Under AC tuning voltages, however, the magnitude of tension reduction has been estimated to be smaller than that of the DC tuning voltages. Therefore, the downward frequency shift that has been observed in our bilayer circular and square membranes is highly likely to be consistent with the reduction of thermally induced tension [24], [28].

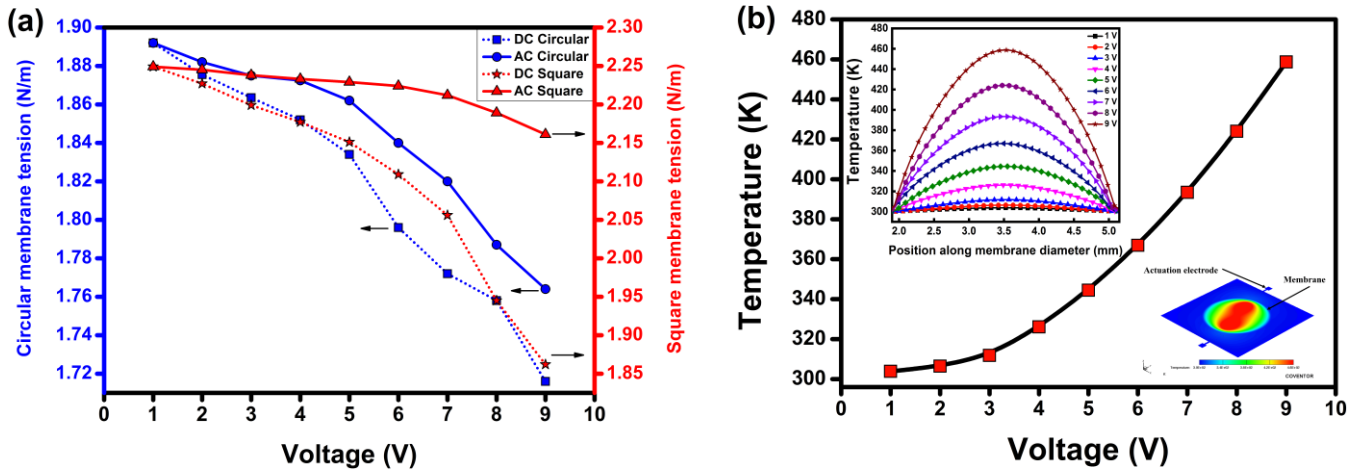

Fig. 6. (**a**) Estimated tension of circular (blue lines) and square (red lines) membranes with respect to the tuning voltage. (**b**) FEA simulations of maximum absolute temperature induced electrothermally in a circular membrane at different tuning voltages. Insets in **b** (top) show the temperature distribution profile along the membrane diameter (top left) and a simulated 3D image of the membrane with heat distributed in the middle (bottom right).

The source of the reduction of the membrane tension could be attributed to the Joule heating phenomenon. When a voltage is applied to the actuation electrodes, electric current will pass through the whole bilayer membrane and generate heat. The generated heat will cause a temperature gradient (ΔT) within the bilayer structure. Since graphene and PMMA have different coefficients of thermal expansion, the temperature gradient within the entire membrane thickness will induce a mechanical strain, hence thermal tension in the membrane. When the thermally induced tension is modified, the mechanical stiffness of the bilayer structure will be altered accordingly. In order to investigate the effect of tuning voltage on the heat generated in the graphene-PMMA membranes, finite element analysis (FEA) simulations of electrothermal tuning have been performed with CoventorWare. The material properties used in the FEA simulations are presented in Table I. In the simulation, a voltage (1 – 9 V) has been applied between the two actuation electrodes (inset bottom right in fig 6b) while applying a film convection boundary condition. In this case, an air flow has been applied to the top and bottom surfaces of the membrane to allow heat to convect away from the model. The simulation has been performed using a convection heat transfer coefficient of 0 W/m^2, a room air temperature (i.e. ambient temperature) of 293 K, and air flow velocity (ambient flow) of 1×10^6 µm/sec. In addition, radiation heat transfer has been considered in the model and hence emissivity of 0.1 has been used. Fig. 6b illustrates the simulation of the maximum absolute temperature and the profile of temperature distributed along the circular membrane diameter (inset) as a function of the tuning voltage. It can be seen that the induced maximum temperature increases significantly with the increase of the tuning voltage. An increase of the maximum absolute temperature of ~ 1.5 % (from 303 to 460 K) has been achieved corresponding to the increase of the tuning voltage from 1 to 9 V. In addition, the simulated profile of the temperature distributed along the membrane diameter has been found to be symmetric (insets in fig. 6b). The part most influenced by the induced temperature seems to be the middle active area of the membrane. In addition, it can be seen that the distributed temperature of the membrane remains constant at the supported area (frame) with a gradual increase at the area in which the membrane is suspended. The temperature reaches its maximum value at the middle part of the membrane, and hence creating a profile with a dome-like shape.

TABLE I
PARAMETERS OF THE MATERIALS USED IN ELECTROTHERMAL SIMULATIONS OF GRAPHENE-PMMA MEMBRANES

Property	Value	
	Graphene	**PMMA**
Diameter	3.5 mm	3.5 mm
Thickness	2.8 nm	370 nm
Young's modulus	1 TPa	3.8 GPa
Poisson's ratio	0.16	0.4
Density	2×10^3 Kg/m^3	1.1×10^3 Kg/m^3
Thermal expansion coefficient	-7×10^{-6} K^{-1}	7.7×10^{-5} K^{-1}
Thermal conductivity	5300 W/mK	0.24 W/mK

From the measurements, calculations and simulations, we can conclude that the increase of the applied voltage from 1 to 9 V leads to a reduction of the membrane tension and hence a downward shift of the resonant frequency. Although the graphene sheet can achieve an extremely high tunability [16], the relatively small tunability that have been observed in our bilayer membranes is possibly because of the fact that the change in tension provided by the polymer supporting layer of PMMA is dominant [17], [29]. In addition, the presence of the PMMA layer, as well as the quality of the contact between metal electrode pads and membrane, might influence the dynamic tuning response of the measured devices. Furthermore, it is possible that the different response of circular and square membranes might be related to the differences in their boundary and clamping conditions.

IV. CONCLUSIONS

We have developed a straightforward and simple process for the fabrication of low frequency electromechanical resonators using a bilayer structure based on a graphene-polymer membrane. Ultra-large multilayer graphene membranes with a thickness of ~2.5 nm supported by a thin film of ~ 370 nm of PMMA have been realized experimentally on a millimeter scale using a simple and reproducible transfer process. The bilayer membranes have been transferred onto circular cavities with a diameter of 3.5 mm and square cavities with a side length of 3 mm. The demonstrated graphene-PMMA resonators have very large diameter (side length) to thickness aspect ratios of ~ 10,000, which allow the resonator to vibrate within the audio range achieving a minimum resonant frequency of ~ 4.5 kHz. The difference in the thermal properties of graphene and PMMA have enabled the resonant frequencies of the bilayer membranes to be tuned electrothermally. The dynamic tuning of the resonators has been investigated electrothermally by applying a combination of AC and DC voltages. The applied AC and DC voltages with ranges of 1 – 5 V and 5 – 9 V have revealed a significant impact on the frequency tuning response. With the increase of the applied voltages, a downward shift of the resonant frequencies accompanied by an increase of the vibration amplitude have been observed. Square membranes have shown better tuning sensitivity than the circular ones for different DC tuning voltage ranges while both types of membranes exhibit almost similar increase in tuning sensitivity for the different AC tuning voltage ranges. The fabrication technique reported in this work can be applied to realize large suspended membranes made from other 2D materials. Furthermore, the obtained results indicate that the graphene-polymer resonators can achieve low frequency vibration within the audible region, holding promise for the development of reliable and high sensitivity transducers for a wide range of acoustic and audio applications such as microphones and hearing aid devices.

ACKNOWLEDGMENT

The authors acknowledge the financial support of UK Engineering and Physical Sciences Research Council (EPSRC).

The Ministry of Higher Education and Scientific Research (MOHESR) of Iraq is acknowledged for the financial support through the PhD scholarship program.

REFERENCES

[1] A. Ishfaque and B. Kim, "Fly Ormia Ochracea Inspired MEMS Directional Microphone: A Review," *IEEE Sens. J.*, vol. 18, no. 5, pp. 1778–1789, Mar. 2018.

[2] R. Bogue, "Recent developments in MEMS sensors: A review of applications, markets and technologies," *Sensor Review*, vol. 33, no. 4. Emerald Group Publishing Limited, pp. 300–304, 09-Sep-2013.

[3] J. Jang, J. H. Jang, and H. Choi, "Biomimetic Artificial Basilar Membranes for Next-Generation Cochlear Implants," *Adv. Healthc. Mater.*, vol. 6, no. 21, p. 1700674, Nov. 2017.

[4] Q. Zhou and A. Zettl, "Electrostatic graphene loudspeaker," *Appl. Phys. Lett.*, vol. 102, no. 22, p. 223109, Jun. 2013.

[5] S. T. Woo *et al.*, "Realization of a high sensitivity microphone for a hearing aid using a graphene−PMMA laminated diaphragm," *ACS Appl. Mater. Interfaces*, vol. 9, no. 2, pp. 1237–1246, Jan. 2017.

[6] Q. Zhou, J. Zheng, S. Onishi, M. F. Crommie, and A. K. Zettl, "Graphene electrostatic microphone and ultrasonic radio," *Proc. Natl. Acad. Sci.*, vol. 112, no. 29, pp. 8942–8946, 2015.

[7] D. Todorović *et al.*, "Multilayer graphene condenser microphone," *2D Mater.*, vol. 2, no. 4, p. 045013, Nov. 2015.

[8] H. Tian *et al.*, "Graphene earphones: Entertainment for both humans and animals," *ACS Nano*, vol. 8, no. 6, pp. 5883–5890, Jun. 2014.

[9] H. Tian, Y. Yang, C. Li, W. T. Mi, M. A. Mohammad, and T. L. Ren, "A flexible, transparent and ultrathin single-layer graphene earphone," *RSC Adv.*, vol. 5, no. 22, pp. 17366–17371, Feb. 2015.

[10] H. Wang and G. Yu, "Direct CVD Graphene Growth on Semiconductors and Dielectrics for Transfer-Free Device Fabrication," *Adv. Mater.*, vol. 28, no. 25, pp. 4956–4975, Jul. 2016.

[11] A. V. Zaretski and D. J. Lipomi, "Processes for non-destructive transfer of graphene: widening the bottleneck for industrial scale production," *Nanoscale*, vol. 7, no. 22, pp. 9963–9969, May 2015.

[12] Y. Chen, X. L. Gong, and J. G. Gai, "Progress and Challenges in Transfer of Large-Area Graphene Films," *Adv. Sci.*, vol. 3, no. 8, p. 1500343, Aug. 2016.

[13] H. C. Lee *et al.*, "Review of the synthesis, transfer, characterization and growth mechanisms of single and multilayer graphene," *RSC Adv.*, vol. 7, no. 26, pp. 15644–15693, Mar. 2017.

[14] R. De Alba *et al.*, "Tunable phonon-cavity coupling in graphene membranes," *Nat. Nanotechnol.*, vol. 11, no. 9, pp. 741–746, Jun. 2016.

[15] C. Chen *et al.*, "Graphene mechanical oscillators with tunable frequency," *Nat. Nanotechnol.*, vol. 8, no. 12, pp. 923–927, Nov. 2013.

[16] C. Chen *et al.*, "Performance of monolayer graphene nanomechanical resonators with electrical readout," *Nat. Nanotechnol.*, vol. 4, no. 12, pp. 861–867, Dec. 2009.

[17] C. Chen *et al.*, "Graphene mechanical oscillators with tunable frequency," *Nat. Nanotechnol.*, vol. 8, no. 12, pp. 923–927, Nov. 2013.

[18] A. M. Van Der Zande *et al.*, "Large-scale arrays of single-layer graphene resonators," *Nano Lett.*, vol. 10, no. 12, pp. 4869–4873, Dec. 2010.

[19] C. N. Lau, W. Bao, and J. Velasco, "Properties of suspended graphene membranes," *Mater. Today*, vol. 15, no. 6, pp. 238–245, Jun. 2012.

[20] A. A. Balandin *et al.*, "Superior thermal conductivity of single-layer graphene," *Nano Lett.*, vol. 8, no. 3, pp. 902–907, Mar. 2008.

[21] G. Liang *et al.*, "Integrated Terahertz Graphene Modulator with 100% Modulation Depth," *ACS Photonics*, vol. 2, no. 11, pp. 1559–1566, Nov. 2015.

[22] B. Vasić, M. M. Jakovljević, G. Isić, and R. Gajić, "Tunable metamaterials based on split ring resonators and doped graphene," *Appl. Phys. Lett.*, vol. 103, no. 1, p. 011102, Jul. 2013.

[23] R. De Alba *et al.*, "Tunable phonon-cavity coupling in graphene membranes," *Nat. Nanotechnol.*, vol. 11, no. 9, pp. 741–746, Jun. 2016.

[24] A. K. Al-Mashaal, G. S. Wood, A. Torin, E. Mastropaolo, M. J. Newton, and R. Cheung, "Dynamic behavior of ultra large graphene-based membranes using electrothermal transduction," *Appl. Phys. Lett.*, vol. 111, no. 24, p. 243503, 2017.

[25] E. Mastropaolo, G. S. Wood, I. Gual, P. Parmiter, and R. Cheung, "Electrothermally actuated silicon carbide tunable MEMS resonators," *J. Microelectromechanical Syst.*, vol. 21, no. 4, pp. 811–821, Aug. 2012.

[26] R. A. Barton *et al.*, "High, size-dependent quality factor in an array of graphene mechanical resonators," *Nano Lett.*, vol. 11, no. 3, pp. 1232–1236, Mar. 2011.

[27] B. Kim *et al.*, "Temperature Dependence of Quality Factor in MEMS Resonators," *J. Microelectromechanical Syst.*, vol. 17, no. 3, pp. 755–766, Jun. 2008.

[28] V. Singh *et al.*, "Probing thermal expansion of graphene and modal dispersion at low-temperature using graphene nanoelectromechanical systems resonators," *Nanotechnology*, vol. 21, no. 16, p. 165204, Apr. 2010.

[29] S. Lee *et al.*, "Electrically integrated SU-8 clamped graphene drum resonators for strain engineering," *Appl. Phys. Lett.*, vol. 102, no. 15, p. 153101, Apr. 2013.